International Journal of Heat and Technology
Vol. 38, No. 2, June, 2020, pp. 377-385
Journal homepage: http://iieta.org/journals/ijht

Magnetohydrodynamic Flow and Heat Transfer of TiO_2-H_2O Nanofluid over Nonlinear Stretching Sheet under the Effects of Nanoparticle Diameter

Asghar Davoudi, Saeid Niazi*, Younes Bakhshan, Jamshid Khorshidi

Department of Mechanical Engineering, Faculty of Engineering, University of Hormozgan, Bandar Abbas 7916193145, Iran

Corresponding Author Email: s.niazi@hormozgan.ac.ir

https://doi.org/10.18280/ijht.380213

Received: 30 July 2019
Accepted: 16 May 2020

Keywords:
TiO_2-H_2O nanofluid, MHD flow, heat transfer, nonlinear stretching sheet, Optimal Homotopy Asymptotic Method

ABSTRACT

The effects of nanoparticle diameter on the magnetohydrodynamic flow and heat transfer of TiO_2-H_2O nanofluid over an exponentially stretching sheet are studied in this paper. It is assumed that the effective viscosity of TiO_2-H_2O nanofluid is a function of nanofluid concentration and nanoparticle diameter by use of new accurate correlation. Therefore, the flow and heat characteristics of TiO_2-H_2O nanofluid near a surface can be found under the effects of nanoparticle diameter for the first time. For this purpose, the governing partial differential equations are transformed to the nonlinear ordinary differential equations using similarity transformations. The resulting equations are solved analytically using Optimal Homotopy Asymptotic Method (OHAM) which is most applicable in the analysis of nonlinear problems. The effects of nanoparticle diameter, nanofluid concentration, and magnetic field on the flow and heat transfer of nanofluid are investigated in detail. The results show that the reduced skin friction is a descending function of nanoparticle diameter. The reduced Nusselt number is a complicated function of magnetic field, nanofluid concentration, and nanoparticle diameter. It can be found that for the specific values of parameters, the curves of reduced Nusselt number with respect to the parameters such as magnetic field and nanofluid concentration have peaks where the maximum of heat transfer occurs.

1. INTRODUCTION

The boundary layer flow and heat transfer of fluid over stretching sheet has significant applications in several engineering processes such as paper production, cooling process of plate in cooling bath, and glass manufacturing. Regarding these applications, the study of boundary layer behavior over a solid surface was started by Sakiadis [1]. Numerous powerful mathematical methods were used to investigate the problem of flow near a surface. Crane [2] used exact similarity solution to study forced convection over a stretching sheet.

Since the pioneering work, effects of various parameters such as magnetic field on the flow and heat transfer of fluid over stretching sheet have been investigated by many authors. For example, the boundary layer flow and heat transfer of fluid in the presence of magnetic field was investigated by Pavlov [3], Ali et al. [4], and Hayat et al. [5]. It can be found from literature that the boundary layer flow and heat transfer of fluid is affected by definition of boundary conditions. The effects of suction and injection on the flow and heat transfer characteristics were studied by Ganji et al. [6] and Abbasi et al. [7].

In several engineering processes, the effects of viscous dissipation and thermal radiation on the flow and heat transfer of fluid in the presence of magnetic field are important. Considering these situations, the effects of magnetic field and viscous dissipation on the flow and heat transfer characteristics of fluid were investigated by many authors [8, 9]. Also, the effects of magnetic field and thermal radiation on the boundary layer flow and heat transfer of fluid were investigated by Hayat et al. [10], Sheikholeslami and Ganji [11] and Malvandi et al. [12].

In the last decades, nanofluids are noticed for high thermal performance in comparison with base fluids. For the first time, the effects of adding nanoparticle to the base fluid were investigated by Choi and Eastman [13]. He showed that the thermal properties of fluid increase by adding nanoparticles for low concentration. Since the pioneering work, various aspects of nanofluids have been studied by many authors [14-17]. Malvandi et al. [18] studied heat transfer enhancement at film boiling of nanofluids over a vertical cylinder. Nallusamy [18] investigated the effects of Al_2O_3-H_2O nanofluid on the overall heat transfer coefficient for a shell and tube heat exchanger. Also, many authors investigated the nanofluid properties. For example, Anoop et al [19], Vajjha et al. [20] and Corcione [21] revealed that thermal conductivity and viscosity of nanofluids depend on the nanoparticle size and nanofluid concentration. Lee et al. [21] investigated the effects of nanoparticle sizes on viscosity for zinc oxide nanoparticle.

In many problems, the results are achieved by solution of nonlinear ordinary differential equations. Therefore, various mathematical methods, such as homotopy perturbation method [22], modified homotopy perturbation method [23], differential transformation method [24], homotopy analysis method [25, 26], and optimal homotopy asymptotic method [27-30] were developed for solving ordinary differential equations. In many problems of fluid mechanic and heat transfer, the governing equations can be transferred to the nonlinear ordinary differential equations. Therefore, several

numerical and analytical methods were used to solve the ordinary differential equations instead of using CFD to solve partial differential equations [31, 32]. The mathematical methods were used to investigate the flow and heat transfer of fluid by Ganji [33], Ganji et al. [34], Ganji and Rajabi [35], Ganji et al. [36], Liao [37], Domairry and Nadim [38], Wang et al. [39], and Liao and Pop [40]. In this study, the governing equations are solved using Optimal Homotopy Asymptotic Method (OHAM) as one of the most appropriate method to solve the nonlinear equations. The authors used this method to solve the governing nonlinear ordinary differential equations of flow and heat transfer of fluid. For example, the governing nonlinear ordinary differential equations of Jeffery-Hamel flow were solved by Esmaeilpour and Ganji [41] using OHAM.

In this paper, the boundary layer of magnetohydrodynamic flow and heat transfer of TiO_2-H_2O nanofluid over an exponentially stretching sheet is investigated analytically under the effects of nanoparticle diameter. The new correlation for viscosity of TiO_2-H_2O nanofluid was derived from experimental data which is used in this paper to investigate the effects of nanoparticle diameter on the flow and heat transfer of nanofluid near a sheet for the first time. In order to investigate the stated problem, the governing nonlinear ordinary differential equations of flow and heat transfer are solved using OHAM which is most applicable in the analysis of nonlinear problems. Consequently, the results of this paper can be useful by the engineers who want to know the effects of nanoparticle diameter on the flow and heat transfer characteristics near surface.

2. DEFINITION OF THE PROBLEM

The flow and heat transfer of nanofluid over a stretching sheet is investigated in this paper where the new accurate correlation for viscosity of TiO_2-H_2O nanofluid as function of nanofluid concentration and nanoparticle diameter is used. The sketch of flow is shown in Figure 1 which is assumed to be created by stretching of the sheet with large force.

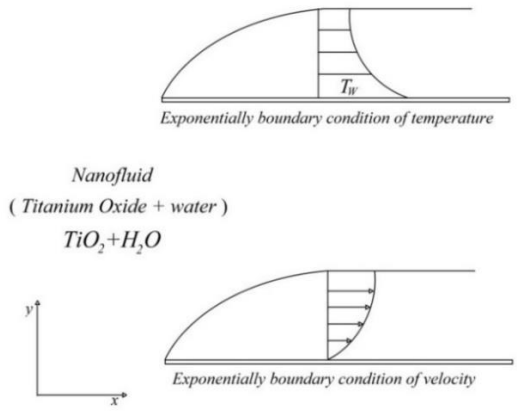

Figure 1. Sketch of the flow past a stretching sheet

3. GOVERNING EQUATIONS

The conservation equations of flow and heat transfer are defined in the following forms [28].

$$\frac{\partial u}{\partial x}+\frac{\partial v}{\partial y}=0 \tag{1}$$

$$u\frac{\partial u}{\partial x}+v\frac{\partial u}{\partial y}=\frac{\mu_{nf}}{\rho_{nf}}\frac{\partial^2 u}{\partial y^2}-\frac{\sigma B_0^2 u}{\rho_{nf}} \tag{2}$$

$$u\frac{\partial T}{\partial x}+v\frac{\partial T}{\partial y}=\frac{k_{nf}}{\rho_{nf}c_{p_{nf}}}\frac{\partial^2 T}{\partial y^2} \tag{3}$$

The effective density, the effective heat capacity, and the effective thermal conductivity of nanofluid are defined as follow where the properties of fluid and particle are presented in Table 1.

Table 1. The physical properties of fluid and particle

	$\rho(kg/m^3)$	C_P(J/kg.K)	k (W/m.K)
Fluid	998.3	4182	0.6
Particle	10490	216.5	429

$$\rho_{nf}=(1-\varphi)\rho_f+\varphi\rho_s \tag{4}$$

$$C_{Pnf}=\frac{(1-\varphi)(\rho C_P)_f+\varphi(\rho C_P)_s}{\rho_{nf}} \tag{5}$$

$$\frac{k_{nf}}{k_f}=\frac{k_p+2k_f-2\varphi(k_f-k_p)}{k_p+2k_f+2\varphi(k_f-k_p)} \tag{6}$$

The effective viscosity of TiO_2-H_2O nanofluid is defined as follows. The below correlation was derived from experimental data [21]. Corcione [21] collected data from different sources. The best-fit for the selected experimental data is found by applying the following empirical correlation with a 1.84% standard deviation of error. The obtained correlation for effective viscosity is acceptable for nanoparticle volume fractions in the range of 0.0001 to 0.071 and temperatures between 293 K and 333 K.

$$\frac{\mu_{nf}}{\mu_f}=\frac{1}{1-34.87\left(\frac{d_p}{d_f}\right)^{-0.3}\varphi^{1.03}} \tag{7}$$

d_p is the diameter of nanoparticle and d_f is defined as follows.

$$d_f=\left(\frac{6M}{N\pi\rho_f}\right)^{1/3} \tag{8}$$

M is the molecular weight of fluid, ρ_f is the density of fluid, and N is the Avogadro number. The above definitions of effective parameters are substituted into Eqns. (1-3). The resulting equations with appropriate boundary conditions are defined as follow.

$$u=u_0e^{\frac{x}{l}},v=0,\ T=T_\infty+T_0e^{\frac{x}{2l}},\qquad at\ y=0$$
$$u\to 0,T\to T_\infty,at\ y\to\infty$$

The non-dimensional similarity transformations are presented in the following forms which are used to achieve

nonlinear ordinary differential equations from governing partial differential equations.

$$u = u_0 e^{\frac{x}{l}} f' \tag{9}$$

$$v = -\sqrt{\frac{\mu u_0}{2l\rho}} e^{\frac{x}{2l}} (f + \eta f') \tag{10}$$

$$T = T_\infty + T_0 e^{\frac{x}{2l}} \theta \tag{11}$$

$$\eta = \sqrt{\frac{\rho u_0}{2\mu l}} e^{\frac{x}{2l}} y \tag{12}$$

The resulting nonlinear ordinary differential equations with appropriate boundary conditions are presented as follow where primes stand for derivatives with respect to η.

$$((1-\varphi) + \varphi(\frac{\rho_p}{\rho_f}))(2f'^2 - ff'') - (\frac{1}{1 - 34.87\left(\frac{d_p}{d_f}\right)^{-0.3} \varphi^{1.03}})f''' + Mf' = 0 \tag{13}$$

$$((1-\varphi) + \varphi(\frac{(\rho C_p)_p}{(\rho C_p)_f}))(f'\theta - f\theta') - \frac{1}{Pr}(\frac{k_p + 2k_f - 2\varphi(k_f - k_p)}{k_p + 2k_f + 2\varphi(k_f - k_p)})\theta'' = 0 \tag{14}$$

$$f = 0, \quad f' = 1, \quad \theta = 1, \quad at\ \eta = 0$$
$$f' = 0, \theta = 0, at\ \eta = \infty$$

M and Pr are defined in the following forms:

$$M = \frac{2\sigma B_0^2 l}{\rho u(0)} \tag{15}$$

$$Pr = \frac{\mu_f}{\rho_f \alpha_f} \tag{16}$$

4. SOLUTION WITH OPTIMAL HOMOTOPY ASYMPTOTIC METHOD

The governing nonlinear ordinary differential Eq. (13) and Eq. (14) are expressed as follow by means of OHAM.

$$(1-P)(f''' + f') - H_1(((1-\varphi) + \varphi(\frac{\rho_p}{\rho_f}))(2f'^2 - ff'') - (\frac{1}{1-34.87\left(\frac{d_p}{d_f}\right)^{-0.3} \varphi^{1.03}})f''' + Mf') = 0 \tag{17}$$

$$(1-P)(\theta' + \theta) - H_2(((1-\varphi) + \varphi(\frac{(\rho C_p)_p}{(\rho C_p)_f}))(f'\theta - f\theta') - \frac{1}{Pr}(\frac{k_p + 2k_f - 2\varphi(k_f - k_p)}{k_p + 2k_f + 2\varphi(k_f - k_p)})\theta'') = 0 \tag{18}$$

f and θ are defined in the following forms, where $f_0, f_1, f_2, \theta_0, \theta_1$, and θ_2 are functions of similarity variable η.

$$f = f_0 + Pf_1 + P^2 f_2 \tag{19}$$

$$\theta = \theta_0 + P\theta_1 + P^2\theta_2 \tag{20}$$

H_1 and H_2 are defined as follow, where C_{11}, C_{12}, C_{21}, and C_{22} are constants.

$$H_1 = PC_{11} + P^2 C_{12} \tag{21}$$

$$H_2 = PC_{21} + P^2 C_{22} \tag{22}$$

The above definitions of H_1, H_2, f, and θ are substituted into Eq. (17) and Eq. (18) and the same powers of P are collected. The resulting ordinary differential equations are solved for the particular case as follows.

$$\varphi = 0.03, \quad M = 0.1, \quad Pr = 7, \quad and\ d_P = 25.10^{-9}$$

The final results are achieved as follow:

$$f_0 = 1 - e^{-\eta} \tag{23}$$

$$\theta_0 = e^{-\eta} \tag{24}$$

$$f_1 = -\frac{0.5488649570C_{11}}{e^{2\eta}} - \frac{0.1708861880\eta C_{11}}{e^{\eta}} - 0.3779787690C_{11} + \frac{0.9268437260C_{11}}{e^{\eta}} \tag{25}$$

$$\theta_1 = -\frac{0.8330600186\eta C_{21}}{e^{\eta}} - \frac{0.1368616102C_{21}}{e^{2\eta}} + \frac{0.1368616102C_{21}}{e^{\eta}} \tag{26}$$

$$f_2 = -\frac{0.01460104460\eta^2 C_{11}^2}{e^{\eta}} + \frac{0.02363448580\eta C_{11}^2}{e^{\eta}} - \frac{0.1875868804\eta C_{11}^2}{e^{2\eta}} + \frac{2.668474856C_{11}^2}{e^{2\eta}} - \frac{0.1708861880\eta C_{11}}{e^{\eta}} - \frac{0.5488649570C_{11}}{e^{2\eta}} - \frac{0.3012527410C_{11}^2}{e^{3\eta}} - \frac{0.1708861880\eta C_{12}}{e^{\eta}} - \frac{0.548864957C_{12}}{e^{2\eta}} + 2.229921768C_{11}^2 - 0.37797877C_{11} - 0.37797877C_{12} - \frac{4.597143883C_{11}^2}{e^{\eta}} + \frac{0.9268437260C_{11}}{e^{\eta}} + \frac{0.9268437260C_{12}}{e^{\eta}} \tag{27}$$

$$\theta_2 = -\frac{0.1368616102C_{22}}{e^{2\eta}} - \frac{0.04677551770\eta C_{21}C_{11}}{e^{2\eta}} + \frac{0.1311330533C_{21}C_{11}}{e^{2\eta}} - \frac{0.6764640543\eta C_{21}^2}{e^{\eta}} - \frac{1.010335272C_{21}^2}{e^{2\eta}} + \frac{0.06781208500C_{21}^2}{e^{3\eta}} - \frac{0.8330600186\eta C_{22}}{e^{\eta}} + \frac{0.3745612577\eta C_{21}C_{11}}{e^{\eta}} - \frac{0.02852298160C_{21}C_{11}}{e^{3\eta}} + \frac{0.3469944973\eta^2 C_{21}^2}{e^{\eta}} - \frac{0.1368616102C_{21}}{e^{2\eta}} - \frac{0.8330600186\eta C_{21}}{e^{\eta}} + \frac{0.1368616102C_{22}}{e^{\eta}} - \frac{0.1026100717C_{21}C_{11}}{e^{\eta}} + \frac{0.9425231870C_{21}^2}{e^{\eta}} + \frac{0.1368616102C_{21}}{e^{\eta}} \tag{28}$$

The above definitions of f_0, f_1, and f_2 are substituted into Eq. (29) to obtain the mathematical formulation for f. This approach is also adopted to achieve θ as follows.

$$f(\eta) = f_0(\eta) + f_1(\eta) + f_2(\eta) \tag{29}$$

$$\theta(\eta) = \theta_0(\eta) + \theta_1(\eta) + \theta_2(\eta) \tag{30}$$

The above definitions of f and θ are substituted into Eq. (13) and Eq. (14) to obtain the results which are named as R_1 and R_2, respectively. G_1 and G_2 are achieved by integration of square errors as follow.

$$G_1(C_{11}, C_{12}\ C_{21}, C_{22}) = \int_0^\infty R_1^2 d\eta \tag{31}$$

$$G_2(C_{11}, C_{12}\ C_{21}, C_{22}) = \int_0^\infty R_2^2 d\eta \tag{32}$$

C_{11}, C_{12}, C_{21}, and C_{22} are constants of the above equations.

$$\frac{\partial G_m}{\partial C_{m1}} = \frac{\partial G_m}{\partial C_{m2}} = \ldots = 0 \tag{33}$$

C_{11}, C_{12}, C_{21}, and C_{22} are achieved as follow from solving the above equations.

$$C_{11} = 0.2242835815,\ C_{12} = -0.3375938152\text{e-}1,$$
$$C_{21} = 1.353843870,\ C_{22} = -0.2069073548$$

Final definitions of f and θ for the stated parameters of d_p, φ, M, and Pr are obtained in the following forms.

$$f(\eta) = -\frac{0.8467887134}{e^{\eta}} - \frac{0.0934408311}{e^{2\eta}} + 0.9553834987 - \frac{0.009436206270\eta}{e^{2\eta}} - \frac{0.0007344781706\eta^2}{e^{\eta}} - \frac{0.06969603203\eta}{e^{\eta}} - \frac{0.01515395427}{e^{3\eta}} \tag{34}$$

$$\theta(\eta) = \frac{3.038648163}{e^{\eta}} - \frac{2.154279614}{e^{2\eta}} - \frac{3.209452900\eta}{e^{\eta}} - \frac{0.01420314982\eta}{e^{2\eta}} + \frac{0.1156314517}{e^{3\eta}} + \frac{0.6360038629\eta^2}{e^{\eta}} \tag{35}$$

5. RESULTS AND DISCUSSION

In this paper, the effects of magnetic field, nanoparticle diameter, and nanofluid concentration on the flow and heat transfer of nanofluid over stretching sheet are investigated. For this purpose, the nonlinear ordinary differential Eq. (13) and Eq. (14) are analytically solved for various values of magnetic field, nanoparticle diameter, and nanofluid concentration. According to Figure 2, the analytical results in the limiting case are in good agreement with the previous published results by Sajid and Hayat [42].

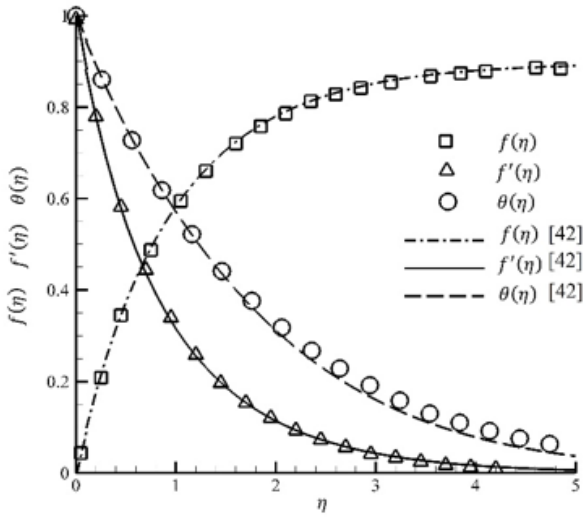

Figure 2. Profile of f(η), θ(η), and f'(η) for the case Pr=1, k_r=1, φ=0, and M=0

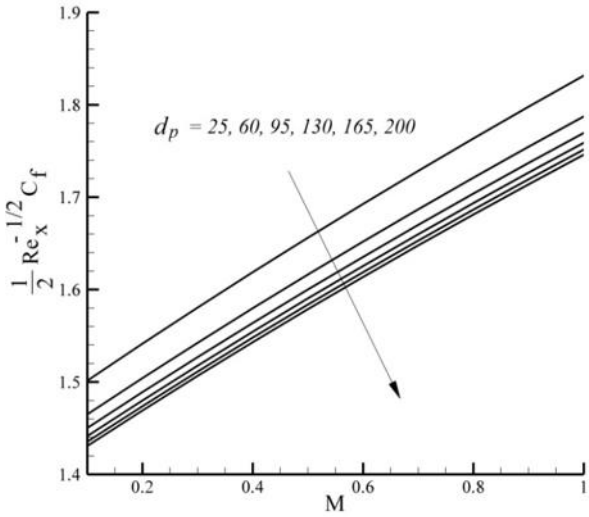

Figure 3. Effects of *M* and *dp* on the reduced skin friction for φ= 0.02

Figures 3-5 show the effects of magnetic field and nanoparticle diameter on the reduced skin friction for the various values of nanofluid concentration. It can be found that the reduced skin friction is an increasing function of magnetic field for all values of nanofluid concentration and nanoparticle diameter. The Lorentz force is an increasing function of magnetic field and it acts opposite to the motion of fluid in this study when the flow of fluid is affected by magnetic field. Therefore, with the increase in magnetic field, the reduced skin friction increases.

Figures 3-5 show that the reduced skin friction is a descending function of nanoparticle diameter. The effective viscosity of TiO_2-H_2O nanofluid is a decreasing function of nanoparticle diameter for each value of nanofluid concentration. Therefore, with the increase in nanoparticle diameter, the reduced skin friction decreases because of reduction in viscosity. It can be found that the reduced skin friction is a nonlinear decreasing function of nanoparticle diameter. The variation of reduced skin friction with respect to the nanoparticle diameter is higher for lower values of nanoparticle diameter. Also, the variation of reduced skin friction with respect to the nanoparticle diameter is higher for

higher values of nanofluid concentration. It means that the size of nanoparticle diameter is more important with the increase in nanofluid concentration.

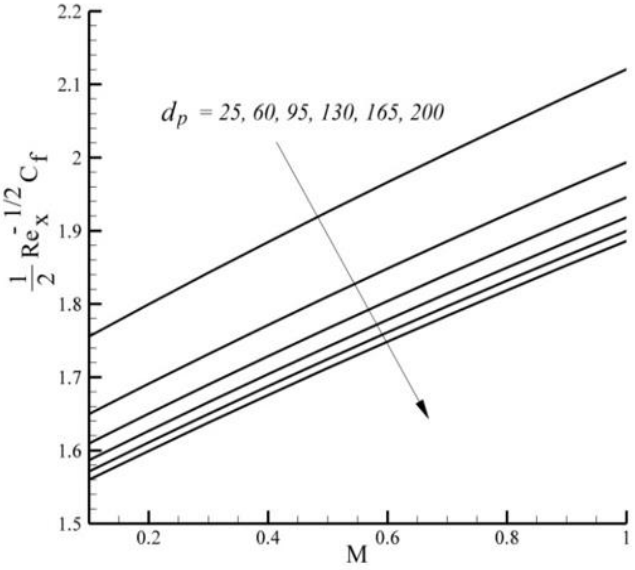

Figure 4. Effects of *M* and *dp* on the reduced skin friction for φ= 0.04

Finally, the general correlation for defining the reduced skin friction as a function of magnetic field, nanoparticle diameter and nanofluid concentration is obtained as follows:

$$\begin{aligned} \textit{Skin friction} \;=\; & (274\phi^2 + 0.02\phi + 1.4) + (66\phi^2 - 2.3\phi + 0.45)M \\ & + (-5.1\phi^2 + 0.12\phi - 0.002)d_p + (-64.07\phi^2 + 6.21\phi - 0.185)M^2 \\ & + (-0.2\phi^2 - 0.02\phi + 0.0006)Md_p + (0.04\phi^2 - 0.001\phi){d_p}^2 \\ & + (0.4\phi^2 - 0.04\phi + 0.001)M^2 d_p + (-0.001\phi^2 + 0.0003\phi)M{d_p}^2 \\ & + (-7.9\times10^{-5}\phi^2 + 1.6\times10^{-6}\phi - 1.9\times10^{-8}){d_p}^3 \end{aligned} \tag{36}$$

By applying the equation of skin friction, the variation of the results with respect to different parameters can be obtained.

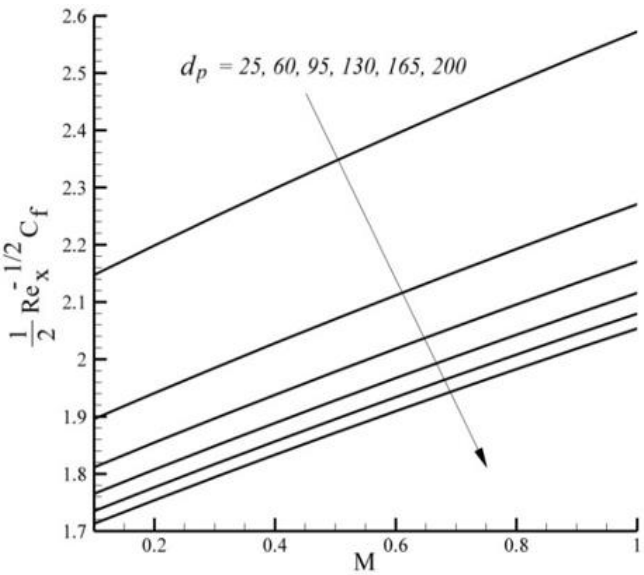

Figure 5. Effects of *M* and *dp* on the reduced skin friction for φ= 0.06

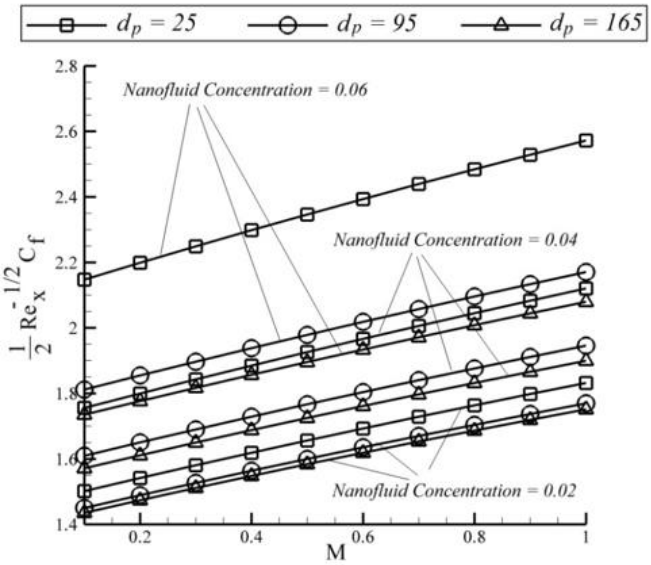

Figure 6. Effects of *φ, M* and *dp* on the reduced skin friction

Figure 6 shows the variation of reduced skin friction with respect to the magnetic field parameter for the various values of nanofluid concentration and nanoparticle diameter. It is shown that the reduced skin friction is an ascending function of nanofluid concentration.

The effective viscosity of TiO_2-H_2O nanofluid is an increasing function of nanofluid concentration for each value of nanoparticle diameter. Therefore, with the increase in nanofluid concentration, the reduced skin friction increases because of increase in viscosity. Also, the variation of reduced skin friction with respect to the nanofluid concentration is higher for higher values of nanofluid concentration.

Figures 7-9 show the effects of magnetic field and nanoparticle diameter on the reduced Nusselt number for the various values of nanofluid concentration. It is shown that the reduced Nusselt number is a complex function of stated parameters. Figure 7 shows that the reduced Nusselt number is an increasing function of nanoparticle diameter where the nanofluid concentration is defined as a small value of 0.02.

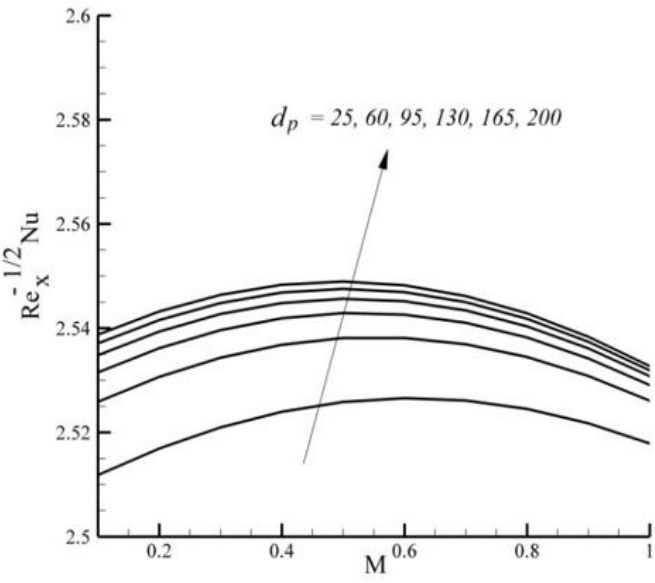

Figure 7. Effects of M and dp on the reduced Nusselt number for φ= 0.02

Also, the variation of reduced Nusselt number with respect to the nanoparticle diameter is higher for lower values of nanoparticle diameter. According to Figure 7, it can be found that the curves of reduced Nusselt number with respect to the magnetic field have peaks which are named critical values in this paper. The reduced Nusselt number with respect to the magnetic field is changed from increasing function to decreasing function by passing critical values. Also, it is shown that critical values of magnetic field are decreasing function of nanoparticle diameter.

Figure 8 shows the effects of magnetic field and nanoparticle diameter on the reduced Nusselt number where the nanofluid concentration is defined as 0.04.

It is shown that the reduced Nusselt number is a nonlinear increasing function of nanoparticle diameter. According to Figure 8, it can be found that the reduced Nusselt number is an increasing function of magnetic field for small value of nanoparticle diameter and the curves of reduced Nusselt number with respect to the magnetic field have peaks for large values of nanoparticle diameter.

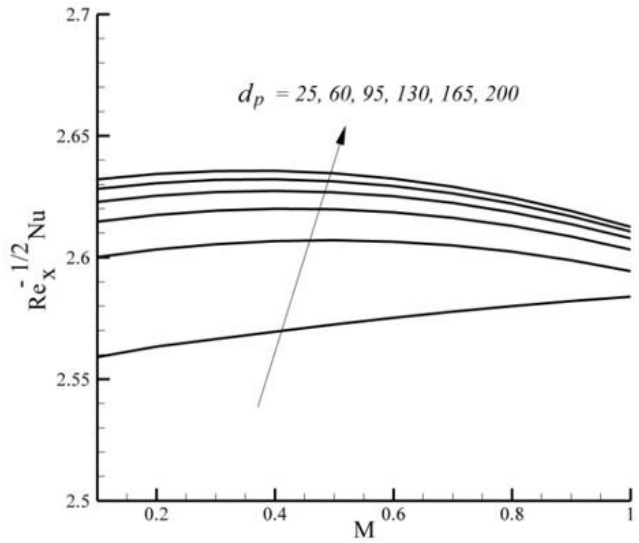

Figure 8. Effects of M and dp on the reduced Nusselt number for φ= 0.02

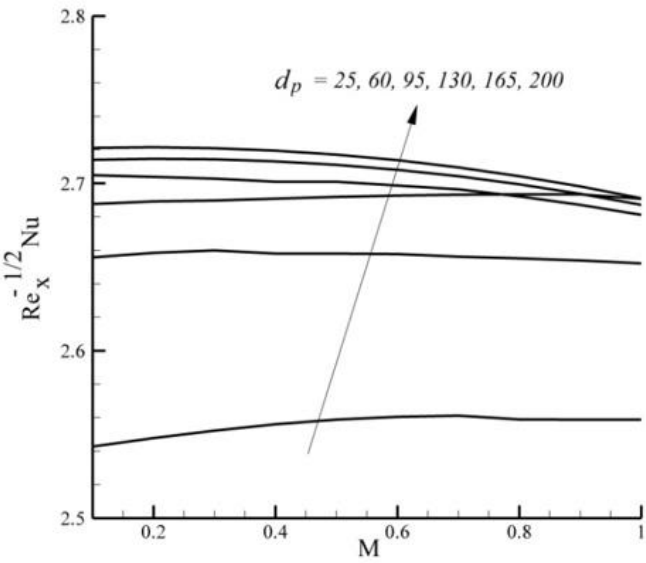

Figure 9. Effects of M and dp on the reduced Nusselt number for φ= 0.02

Therefore, the reduced Nusselt number is changed from increasing function of magnetic field to decreasing function of magnetic field by passing the peaks for large values of nanoparticle diameter.

Figure 9 shows the effects of magnetic field and nanoparticle diameter on the reduced Nusselt number where the nanofluid concentration is defined as 0.06. According to Figure 9, it can be found that the reduced Nusselt number is a complicated function of nanoparticle diameter. The reduced Nusselt number is an increasing function of nanoparticle diameter for small values of magnetic field whereas it is a complicated function of nanoparticle diameter for large values of magnetic field. Therefore, the diameter of nanoparticle is more important where the nanofluid is made by high concentration.

Figure 10 shows comparison between the curves of reduced Nusselt number with respect to the magnetic field parameter for the various values of nanofluid concentration and nanoparticle diameter. It can be found that the reduced Nusselt number is an increasing function of nanofluid concentration for large values of nanoparticle diameter. According to Figure 10, the reduced Nusselt with respect to the nanofluid concentration is changed from increasing function to decreasing function by passing through the critical value of nanofluid concentration for small values of nanoparticle diameter.

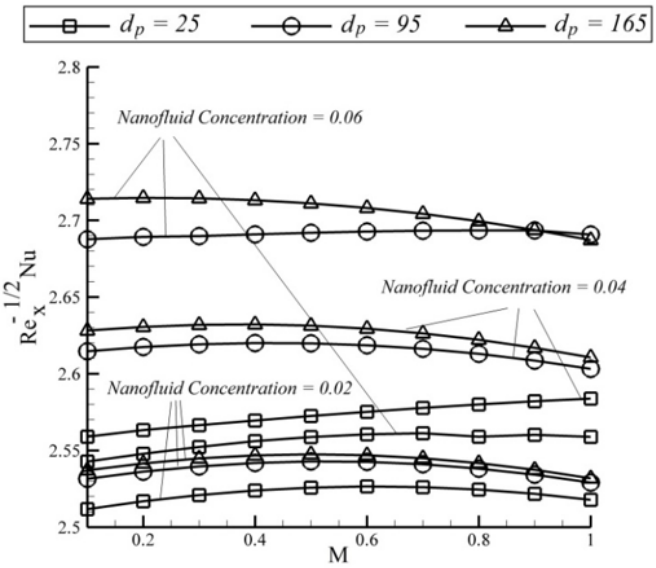

Figure 10. Effects of *φ, M* and *dp* on the reduced Nusselt number

The results in this paper show variations of reduced skin friction and reduced Nusselt number with respect to the parameters such as magnetic field, nanofluid concentration, and nanoparticle diameter. The maximum of heat transfer and skin friction can be controlled by use of these results which are investigated in this paper.

6. CONCLUSION

In the present work, the effects of nanoparticle diameter, nanofluid concentration, and magnetic field on the flow and heat transfer characteristics of TiO_2-H_2O nanofluid over an exponentially stretching sheet are investigated by use of new

accurate correlation for viscosity which was derived from experimental data. The governing partial differential equations are first transformed into nonlinear ordinary differential equations and the resulting equations are solved analytically using Optimal Homotopy Asymptotic Method. It is found that, the reduced skin friction is an ascending function of magnetic field parameter and nanofluid concentration, whereas it is a nonlinear decreasing function of nanoparticle diameter. It is shown that the variation of reduced skin friction with respect to the nanoparticle diameter increases with the increase in nanofluid concentration and it increases with the decrease in nanoparticle diameter. According to this study, the reduced Nusselt number is an increasing function of nanoparticle diameter for small values of nanofluid concentration and the variation of reduced Nusselt number with respect to the nanoparticle diameter is a function of magnetic field for large values of nanofluid concentration. The results show that the variation of reduced Nusselt number with respect to the nanofluid concentration is a function of nanoparticle diameter. It is shown that the reduced Nusselt number is a nonlinear increasing function of nanofluid concentration for large values of nanoparticle diameter and the curves of reduced Nusselt number with respect to the nanofluid concentration have peaks for small values of nanoparticle diameter. According to this paper, the variation of reduced Nusselt number with respect to the magnetic field is a complicated function of nanofluid concentration, nanoparticle diameter, and the value of magnetic field which is investigated in detail.

REFERENCES

[1] Sakiadis, B.C. (1961). Boundary-layer behavior on continuous solid surfaces: I. Boundary-layer equations for two-dimensional and axisymmetric flow. AIChE Journal, 7(1): 26-8. https://doi.org/10.1002/aic.690070108

[2] Crane, L.J. (1970). Flow past a stretching plate. Zeitschrift für angewandte Mathematik und Physik ZAMP, 21: 645-7. https://doi.org/10.1007/BF01587695

[3] Pavlov, K.B. (1974). Magnetohydrodynamic flow of an incompressible viscous fluid caused by deformation of a plane surface. Magnetohydrodynamics, 4: 507-10. http://doi.org/10.22364/mhd

[4] Ali, F.M., Nazar, R., Arifin, N.M., Pop, I. (2011). MHD boundary layer flow and heat transfer over a stretching sheet with induced magnetic field. Heat and Mass Transfer, 47: 155-62. https://doi.org/10.1007/s00231-010-0693-4

[5] Hayat, T., Khan, M.I., Waqas, M., Alsaedi, A., Yasmeen, T. (2017). Diffusion of chemically reactive species in third grade fluid flow over an exponentially stretching sheet considering magnetic field effects. Chinese Journal of Chemical Engineering, 25(3): 257-63. https://doi.org/10.1016/j.cjche.2016.06.008

[6] Ganji, D.D., Abbasi, M., Rahimi, J., Gholami, M., Rahimipetroudi, I. (2014). On the MHD squeeze flow between two parallel disks with suction or injection via HAM and HPM. Frontiers of Mechanical Engineering, 9: 270-80. https://doi.org/10.1007/s11465-014-0303-0

[7] Abbasi, M., Khaki, M., Rahbari, A., Ganji, D.D., Rahimipetroudi, I. (2015). Analysis of MHD flow characteristics of an UCM viscoelastic flow in a permeable channel under slip conditions. Journal of the Brazilian Society of Mechanical Sciences and Engineering, 38: 977-988. https://doi.org/10.1007/s40430-015-0325-5

[8] Sheikholeslami, M., Ashorynejad, H.R., Ganji, D.D., Kolahdooz, A. (2011). Investigation of rotating MHD viscous flow and heat transfer between stretching and porous surfaces using analytical method. Mathematical Problems in Engineering, 2011: 1-17. https://doi.org/10.1155/2011/258734

[9] Sheikholeslami, M., Abelman, S., Ganji, D.D. (2014). Numerical simulation of MHD nanofluid flow and heat transfer considering viscous dissipation. International Journal of Heat and Mass Transfer, 79: 212-222. https://doi.org/10.1016/j.ijheatmasstransfer.2014.08.004

[10] Hayat, T., Sajid, M., Abbas, Z., Asghar, S. (2007). The influence of thermal radiation on MHD flow of a second grade fluid. International Journal of Heat and Mass Transfer, 50(5-6): 931-41. https://doi.org/10.1016/j.ijheatmasstransfer.2006.08.014

[11] Sheikholeslami, M., Ganji, D.D. (2015). Unsteady nanofluid flow and heat transfer in presence of magnetic field considering thermal radiation. Journal of the Brazilian Society of Mechanical Sciences and Engineering, 37: 895-902. https://doi.org/10.1007/s40430-014-0228-x

[12] Malvandi, A., Hedayati, F., Domairry, G. (2013). Stagnation point flow of a nanofluid toward an exponentially stretching sheet with nonuniform heat generation/absorption. Journal of Thermodynamics, 2013: 12. https://doi.org/10.1155/2013/764827

[13] Choi, S.U.S., Eastman, J.A. (1995). Enhancing Thermal Conductivity of Fluids with Nanoparticles. In: Siginer DA, Wang HP, editors Developments and Applications of Non-Newtonian Flows, vols 31/MD–66 New York, NY, FED: ASME Publ, 99-105.

[14] Dogonchi, A.S., Divsalar, K., Ganji, D.D. (2016). Flow and heat transfer of MHD nanofluid between parallel plates in the presence of thermal radiation. Computer Methods in Applied Mechanics and Engineering, 310: 58-76. https://doi.org/10.1016/j.cma.2016.07.003

[15] Asgharsedighi, A., Mirzamohammad, A. (2018). Investigation of magnetohydrodynamic flow and heat transfer of Ag–H_2O nanofluid over exponentially stretching sheet in presence of radiation using OHAM. Journal of Nanofluids, 7(4): 801-808. https://doi.org/10.1166/jon.2018.1485

[16] Karambasti, B.M., Sedighi, A.A. (2019). Numerical investigation of flow and heat transfer of Al_2O_3-water nanofluid in a channel partially filled with porous media considering effects of temperature on the properties of nanofluid. Advanced Science, Engineering and Medicine, 11(9): 817-22. https://doi.org/10.1166/asem.2019.2425

[17] Sedighi, A.A., Deldoost, Z., Mahjoob Karambasti, B. (2019). Flow and heat transfer of nanofluid in a channel partially filled with porous media considering turbulence effect in pores. Canadian Journal of Physics, 98(3): 297-302. https://doi.org/10.1139/cjp-2018-0971

[18] Malvandi, A., Heysiattalab, S., Ganji, D.D. (2016). Thermophoresis and Brownian motion effects on heat transfer enhancement at film boiling of nanofluids over a vertical cylinder. Journal of Molecular Liquids, 216: 503-9. https://doi.org/10.1016/j.molliq.2016.01.030

[19] Anoop, K.B., Sundararajan, T., Das, S.K. (2009). Effect of particle size on the convective heat transfer in

nanofluid in the developing region. International Journal of Heat and Mass Transfer, 52(9-10): 2189-2195. https://doi.org/10.1016/j.ijheatmasstransfer.2007.11.063
[20] Vajjha, R.S., Das, D.K., Kulkarni, D.P. (2010). Development of new correlations for convective heat transfer and friction factor in turbulent regime for nanofluids. International Journal of Heat and Mass Transfer, 53(21-22): 4607-4718. https://doi.org/10.1016/j.ijheatmasstransfer.2010.06.032
[21] Corcione, M. (2011). Empirical correlating equations for predicting the effective thermal conductivity and dynamic viscosity of nanofluids. Energy Conversion and Management, 52(1): 789-793. https://doi.org/10.1016/j.enconman.2010.06.072
[22] He, J.H. (2005). Application of homotopy perturbation method to nonlinear wave equations. Chaos, Solitons & Fractals, 26(3): 695-700. https://doi.org/10.1016/j.chaos.2005.03.006
[23] Marinca, V. (2006). Application of modified homotopy perturbation method to nonlinear oscillations. Archives of Mechanics, 58: 241-256.
[24] Zhou, J.K. (1986). Differential Transformation and Its Applications for Electrical Circuits. Wuhan, China: Huazhong University Press.
[25] Liao, S.J. (1992). The proposed homotopy analysis technique for the solution of nonlinear problems: Shanghai Jiao Tong University.
[26] Liao, S.J. (2004). Beyond Perturbation: introduction to homotopy analysis method. Chapman and Hall/CRC, 57(5): 25. https://doi.org/10.1115/1.1818689
[27] Tahani, M., Sedighi, A., Deldoost, Z. (2017). Analytical investigation of magnetohydrodynamics flow and heat transfer over exponentially stretching sheet in presence of thermal radiation using OHAM. 9th International Exergy, Energy and Environment Symposium (IEEES-9).
[28] Sedighi, A.A. (2017). Steady boundary layer magnetohydrodynamic viscous flow and heat transfer of nanofluid over stretching sheet in presence of radiation and heat source. Journal of Nanofluids, 6(6): 1206-14. https://doi.org/10.1166/jon.2017.1402
[29] Abdollahzadeh, M., Sedighi, A.A., Esmaeilpour, M. (2018). Boundary layer and heat transfer analysis in liquid film of nanofluid over an unsteady stretching sheet. Journal of Nanofluids, 7(2): 371-377. https://doi.org/10.1166/jon.2018.1442
[30] Sedighi, A.A., Deldoost, Z. (2018). Effects of magnetic field and thermal radiation on the flow and heat transfer characteristics of nanofluid over sheet. Journal of Nanofluids, 7(1): 141-148. https://doi.org/10.1166/jon.2018.1436
[31] Sedighi, A.A., Bazargan, M. (2019). A CFD analysis of the pollutant dispersion from cooling towers with various configurations in the lower region of atmospheric boundary layer. Science of the Total Environment, 696: 133939. https://doi.org/10.1016/j.scitotenv.2019.133939
[32] Sedighi, A.A., Deldoost, Z., Karambasti, B.M. (2020). Effect of thermal energy storage layer porosity on performance of solar chimney power plant considering turbine pressure drop. Energy, 194: 116859. https://doi.org/10.1016/j.energy.2019.116859
[33] Ganji, D.D. (2006). The application of He's homotopy perturbation method to nonlinear equations arising in heat transfer. Physics Letters A, 355(4-5): 337-341. https://doi.org/10.1016/j.physleta.2006.02.056
[34] Ganji, D.D., Ganji, Z.Z., Ganji, H.D. (2011). Determination of temperature distribution for annular fins with temperature dependent thermal conductivity by HPM. Thermal Science, 15(suppl. 1): 111-115. https://doi.org/10.2298/TSCI11S1111G
[35] Ganji, D.D., Rajabi, A. (2006). Assessment of homotopy–perturbation and perturbation methods in heat radiation equations. International Communications in Heat and Mass Transfer, 33(3): 391-400. https://doi.org/10.1016/j.icheatmasstransfer.2005.11.001
[36] Ganji, D.D., Hosseini, M.J., Shayegh, J. (2007). Some nonlinear heat transfer equations solved by three approximate methods. International Communications in Heat and Mass Transfer, 34(8): 1003-1016. https://doi.org/10.1016/j.icheatmasstransfer.2007.05.010
[37] Liao, S.J. (1999). An explicit, totally analytic approximate solution for Blasius' viscous flow problems. International Journal of Non-Linear Mechanics, 34(4): 759-778. https://doi.org/10.1016/S0020-7462(98)00056-0
[38] Domairry, G., Nadim, N. (2008). Assessment of homotopy analysis method and homotopy perturbation method in non-linear heat transfer equation. International Communications in Heat and Mass Transfer, 35(1): 93-102. https://doi.org/10.1016/j.icheatmasstransfer.2007.06.007
[39] Wang, C., Liao, S.J., Zhu, J. (2003). An explicit solution for the combined heat and mass transfer by natural convection from a vertical wall in a non-Darcy porous medium. International Journal of Heat and Mass Transfer, 46(25): 4813-4822. https://doi.org/10.1016/S0017-9310(03)00347-8
[40] Liao, S.J., Pop, I. (2004). Explicit analytic solution for similarity boundary layer equations. International Journal of Heat and Mass Transfer, 47(1): 75-85. https://doi.org/10.1016/S0017-9310(03)00405-8
[41] Esmaeilpour, M., Ganji, D.D. (2010). Solution of the Jeffery–Hamel flow problem by optimal homotopy asymptotic method. Computers & Mathematics with Applications, 59(11): 3405-3511. https://doi.org/10.1016/j.camwa.2010.03.024
[42] Sajid, M., Hayat, T. (2008). Influence of thermal radiation on the boundary layer flow due to an exponentially stretching sheet. International Communications in Heat and Mass Transfer, 35(3): 347-356. https://doi.org/10.1016/j.icheatmasstransfer.2007.08.006

NOMENCLATURE

B_0	Uniform magnetic field, T
C	Constant
C_p	Specific heat at constant pressure, J/kg.K
Ec	Eckert number
f	Dimensionless stream function
H	Auxiliary function for P
k	Thermal conductivity, W/m.K
K_r	Thermal radiation parameter

k^*	Mean absorption coefficient
M	Magnetic field parameter
MHD	Magnetohydrodynamic
P	Embedding parameter
Pr	Prandtl number
Q'	Heat source parameter
Q	Heat source
q_r	Radiative heat flux
T	Temperature, K
T_∞	Temperature far away from the wall, K
T_0	Reference temperature, T
u	Velocity component in x direction, m/s
u_0	Reference velocity, m/s
v	Velocity component in y direction, m/s

Greek symbols

α	Thermal diffusivity (m^2/s)
η	Similarity variable
θ	Dimensionless temperature
μ	Viscosity (kg/m.s)
ρ	Density (kg/m^3)
σ	Electrical conductivity of the fluid
σ^*	Stefan–Boltzmann constant ($W/m^2.K^4$)
Φ	Nanoparticle concentration

Subscripts

f	Fluid
Nf	Nanofluid
P	Particle